research articles Journal of proteome research

Combined Comparative and Chemical Proteomics on the Mechanisms of *levo*-Tetrahydropalmatine-Induced Antinociception in the Formalin Test

Chen Wang,[†,‡,§] Jiangrui Zhou,[||] Shuowen Wang,[†,§] Mingliang Ye,[‡] Chunlei Jiang,[||] Guorong Fan,[*,†,§] and Hanfa Zou[*,‡]

Department of Pharmaceutical Analysis, School of Pharmacy, Second Military Medical University, No.325 Guohe Road, Shanghai 200433, People's Republic of China, Division of Biotechnology, Dalian Institute of Chemical Physics, CAS, No.457 Zhongshan Road, Dalian 116023, People's Republic of China, Laboratory of Stress Medicine, Department of Nautical Medicine, Second Military Medical University, No.800 Xiangyin Road, Shanghai 200433, People's Republic of China, and Shanghai Key Laboratory for Pharmaceutical Metabolite Research, No.325 Guohe Road, Shanghai 200433, People's Republic of China

Received February 10, 2010

This study investigated the mechanisms involved in the antinociceptive action induced by levo-tetrahydropalmatine (L-THP) in the formalin test by combined comparative and chemical proteomics. Rats were pretreated with L-THP by the oral route (40 mg/kg) 1 h before formalin injection. The antinociceptive effect of L-THP was shown in the first and second phases of the formalin test. To address the mechanisms by which L-THP inhibits formalin-induced nociception in rats, the combined comparative and chemical proteomics were applied. A novel high-throughput comparative proteomic approach based on 2D-nano-LC−MS/MS was applied to simultaneously evaluate the deregulated proteins involved in the response of L-THP treatment in formalin-induced pain rats. Thousands of proteins were identified, among which 17 proteins survived the stringent filter criteria and were further included for functional discussion. Two proteins (Neurabin-1 and Calcium-dependent secretion activator 1) were randomly selected, and their expression levels were further confirmed by Western Blots. The results matched well with those of proteomics. In the present study, we also described the development and application of L-THP immobilized beads to bind the targets. Following incubation with cellular lysates, the proteome interacting with the fixed L-THP was identified. The results of comparative and chemical proteomics were quite complementary. Although the precise roles of these identified moleculars in L-THP-induced antinociception need further study, the combined results indicated that proteins associated with signal transduction, vesicular trafficking and neurotransmitter release, energy metabolism, and ion transport play important roles in L-THP-induced antinociception in the formalin test.

Keywords: 2-D nano LC • proteomics • chemoproteomics • tetrahydropalmatine

1. Introduction

Corydalis yanhusuo also called *Rhizoma corydalis* is well-known as an analgesic agent in traditional Chinese medicines for thousands of years. *Rhizoma corydalis* is widely used to treat spastic pain, abdominal pain, and pain due to injuries. Levo-tetrahydropalmatine (L-THP, Figure 1) which is one of the main active ingredients isolated from *Corydalis yanhusuo*, was demonstrated to have excellent analgesic effects and has been in use in clinical practice for years in China. L-THP has been verified as a dopamine (DA) receptor antagonist, and it has affinity for opiate receptors.[1,2] In the past decades, the antinociceptive mechanisms of L-THP were explored by many Chinese scientists, and they found that L-THP and its analogues can mediate the striatum/Nucleus accumbens (NAc)-arcuate nucleus (Ar) -Periaqueductal gray (PAG) pathway through blockade of D2 dopamine receptors to regulate nociception.[3] The rat striatum is known to have a higher density of D2 dopamine receptors in comparison with other brain tissues.[4,5] Our previous studies have shown that the striatum exhibited

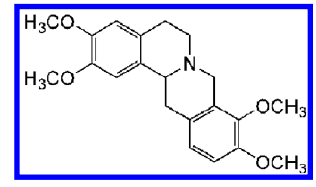

Figure 1. Chemical structure of L-THP.

* To whom correspondence should be addressed. Professor Guorong Fan, School of Pharmacy, Second Military Medical University, No. 325 Guohe Road, Shanghai 200433, P.R. China. Tel.: +86-21-8187-1260, Fax: +86-21-8187-1260, E-mail address: Guorfan@yahoo.com.cn (G.R. Fan); hanfazou@dicp.ac.cn (H. Zou).

† School of Pharmacy, Second Military Medical University.

‡ Dalian Institute of Chemical Physics.

§ Shanghai Key Laboratory for Pharmaceutical Metabolite Research.

|| Department of Nautical Medicine, Second Military Medical University.

10.1021/pr1001274

Published on Web 04/01/2010

the highest concentration of L-THP among the six brain regions, namely the cortex, cerebellum, diencephalons, brain stem and hippocampus.[6,7] All this evidence suggested that striatum plays an important role in antinocecptive effects of L-THP. In addition, L-THP can markedly reduce the concentrations of glutamic acid (Glu) and the ratio of Glu/GABA in mice with cerebral ischemia.[8] However, the detailed molecular bases of L-THP-induced antinociception on the proteome level remain largely unexplored.

Over the last decades, remarkable progress has been achieved regarding the understanding of the neurophysiologic and neuropharmacological bases of pain. However, the problem of understanding of molecular basis of neurophysiologic and neuropharmacological pain and in the development of effective strategies for early diagnosis and for treatment still remains quite a mystery. Proteins are central to our understanding of cellular function and disease processes. Proteomics in general deals with the large-scale determination of gene and cellular function directly at the proteome level, and the MS-based proteomics has established itself as an indispensable technology to interpret the information encoded in proteome.[9] The proteomic approach is widely applied nowadays in the development of novel biomarker candidates for early detection of disease and identification of new targets for therapeutics, mainly by delineation of protein expression changes depending on factors such as the organism's physiological state and the stage of development of disease.[10−12] However, traditional proteomics methodology provides information for abundant proteins but only provides limited information for proteins with low abundance.[13,14] Chemical proteomics, which uses small molecules as baits to fish for interacting proteins, has emerged as a powerful way to investigate the interacting proteome.[15,16] By taking a chemical proteomic approach, only a manageable fraction of the proteome interacting with the fixed small molecules will be collected and analyzed, and this approach greatly reduces the complexity of a certain proteome and thus enhances the ability to detect and to characterize low-abundance proteins. Furthermore, chemical proteomics becomes a direct readout for the characterization of target proteins and related recognition mechanisms of many drugs whose targets are still unclear, especially for compounds of natural origin.[17]

In the present study, we employed a high-throughput comparative proteomic approach based on online 2D-nano-LC−MS/MS to investigate the possible signaling pathways involved in the process of L-THP-induced antinociception in the formalin test. A chemical proteomic approach was applied to detect the proteome interacting with the fixed L-THP. The main purpose of the present study was to explore the detailed molecular bases of L-THP-induced antinociception on the proteome level with the combined comparative and chemical proteomics, so as to get better knowledge of antinociceptive mechanism of L-THP.

2. Experimental Section

2.1. Materials. L-THP sulfate (optical purity ≥99.5%) was provided by Nanning Pharmaceuticals (Guangxi, China). Dithiothreitol (DTT), iodoacetamide (IAA), Triton X-100, PMSF, and Tris were purchased from Sino-American Biotechnology Corporation (Beijing, China). Urea, ammonium acetate, trypsin, and Protease inhibitor cocktail (EDTA free) were purchased from Roche (Penzberg, Germany). Anti-CAPS1 and antineurabin-1 were purchased from Abcam (Cambridge, U.K.). Anti-β-actin antibody was purchased from Cell Signal Technology (Danvers, MA). Antirabbit IgG labeled with HRP was purchased from Santa Cruz Biotechnology (Santa Cruz, CA). Sepharose CL-4B was purchased from Amersham Biosciences. HPLC-grade acetonitrile was obtained from Merck KGaA (Darmstadt, German). Double-distilled water was used for the preparation of all solutions.

Sprague−Dawley (180−220 g, male) rats were purchased from Shanghai SLAC Laboratory Animal Co. Ltd. (Shanghai, China). All experiments followed the Guidelines on Ethical Standards for Investigation of Experiment Pain in Animals[18] and were approved by our local Ethics Committee. Furthermore, every effort was done to minimize pain and suffering in animals, and the number of rats used was the minimal required to obtain significant statistical power.

2.2. Formalin Test. SD rats were fed with certified standard diet and tap water *ad libitum*. Temperature and humidity were regulated at 21−23 °C and 30−60%, respectively. A light/dark cycle of 12 h on/12 h off was established. After one week of acclimatization, the rats were divided randomly into four groups ($n = 8$/group). Group A received vehicle (normal saline) 1 h prior to normal saline injection; Group B received L-THP (40 mg/kg, normal saline) 1 h prior to normal saline injection; Group C (CONs) received vehicle (normal saline) 1 h prior to formalin injection; Group D (L-THPs) received L-THP (40 mg/kg, normal saline) 1 h prior to formalin injection. A formalin solution (5% in normal saline; 50 μL/paw) or normal saline was injected into the right-hind paw plantar surface using 30-guage needle, and the rats were individually placed in transparent observation chambers, as previously described.[19] The time rat spent in licking the injected paw was recorded and expressed as the total licking time in the early phase (0−5 min) and late phase (15−30 min) after formalin injection.

2.3. Sample Preparation for Comparative Proteomic Study. At the end of the formalin test experiments, the animals were sacrificed by decapitation, the striatum was obtained and stored at −80 °C until use. The frozen striatum was homogenized in 1 mL of lysis buffer (8 M urea, 50 mM Tris-HCl, pH 7.5, 0.25% v/v Triton X-100, 1 mM PMSF, 1 mM DTT, 1× protease inhibitor cocktail). The homogenate was centrifuged at 20 000 rpm for 30 min at 4 °C, and the supernatant was mixed with five volumes of precipitation buffer (ethanol: acetone: glacial acetic acid 50:50:0.1). Precipitant was carried out at −20 °C overnight. After washed three times with cold acetone, the pellet was dissolved in denature buffer (8 M urea, 50 mM Tris-HCl, pH 8.3) in a concentration about 1 mg/mL. The sample was reduced by DTT at 37 °C for 2 h and alkylated by iodoacetamide in the dark at room temperature for 40 min. Then the solution was diluted to 1 M urea with 50 mM Tris-HCl (pH 8.3). Finally, trypsin was added at an enzyme-to-substrate of 1/25 (w/w) and incubated at 37 °C overnight. The digested mixture was loaded on a homemade C_{18} solid-phase cartridge (20 mg, 1 mL) previously conditioned with 1.5 mL (0.5 mL × 3) acetonitrile and 1.5 mL (0.5 mL × 3) water (containing 0.1% TFA), then the cartridge was washed with 1.5 mL (0.5 mL × 3) water (containing 0.1% TFA) and eluted with 1 mL (0.5 mL × 2) 80% acetonitrile (containing 0.1% TFA). The elution was SpeedVaced and stored at −80 °C before 2D-nano-LC−MS/MS analysis.

2.4. Preparation of Affinity Matrix. The synthesis of the amino-tetrahydropalmatine (NH_2-THP) was according to the literature[20] (Figure 2). Briefly, to a stirred solution of L-THP (2 g in 20 mL of glacial acetic acid), 4 mL of conc. HNO_3 was

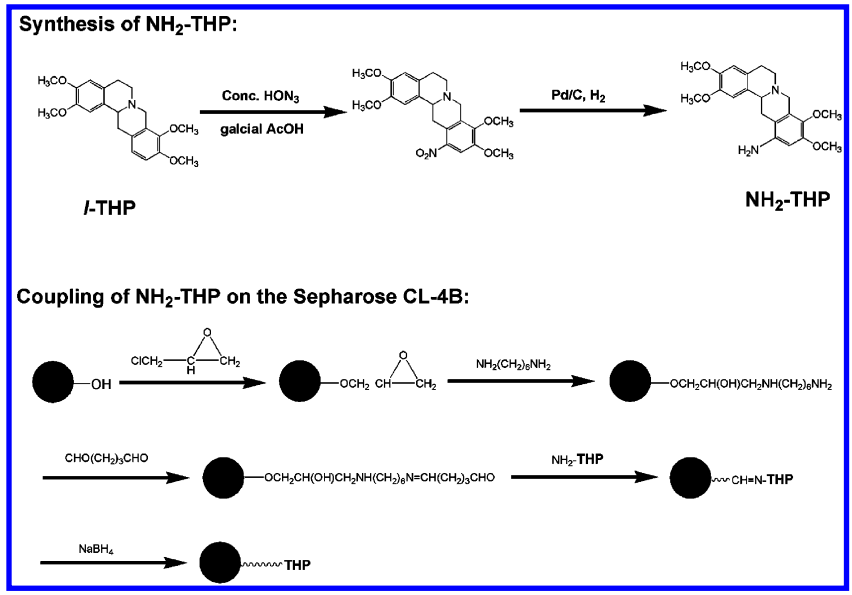

Figure 2. Scheme of synthesis NH_2-THP and coupling of NH_2-THP onto the Sepharose CL-4B.

added dropwise at 0 °C and the mixture stirred for 30 min at ambient temperature. The mixture was then poured into 50 mL of water and extracted with $CHCl_3$. The $CHCl_3$ extraction was washed with water and the solvent was removed *in vacuo*. The product obtained was chromatographed over a silica gel column (3.2 cm id × 9 cm, 300−400 mesh). Elution with mixture of CH_2Cl_2 and MeOH was monitored by TLC and about 600 mg of nitro-tetrahydropalmatine was obtained. Finally, the nitro-tetrahydropalmatine was reduced under reductive condition (H_2−Pd/C) in CH_3OH. The produce obtained was filtered off and dried *in vacuo*. The residue was purified by recrystallization and 340 mg of the NH_2-THP was obtained. The chemical structure of NH_2-THP was identified according to the ESI-MS (Varian, Palo Alto, CA), ^1H and ^{13}C NMR (Bruker, Karlsruhe, Germany) data (Supporting Information 1).

The coupling of NH_2-THP on the Sepharose CL-4B matrix was according to the literature with modifications[21] (Figure 2). In detail, 6 mL of Sepharose CL-4B was washed and mixed with 10 mL of 1 M NaOH and 2 mL of epichlorohydrin. The suspension was mixed by rotation for 2 h at 40 °C and the gel was washed with anhydrous ethanol and water, respectively. After that, 0.3 g 1,6-diaminohexane (dissolved in 10 mL of water) was added dropwise, the mixture stirred for 4 h at 55 °C. Then the drained gel was rotated with 3 mL 25% (v/v) glutaraldehyde in 10 mL of H_2O at 55 °C for 4 h. Finally, the gel was washed and drained. For immobilization, 20 mg of NH_2-THP dissolved in 15 mL of dimethylformamide (DMF)/CH_3OH (1:1, v/v) and activated gel was resuspended in and incubated at 55 °C for 36 h. After that, 50 mg $NaBH_4$ was added and reacted for further 10 h. The mixture was filtered and washed with DMF/CH_3OH (1:1, v/v), ethanol and water. The uncoupled of NH_2-THP was determined by HPLC performed on a reversed-phase Diamonsil™ C_{18} (200 × 4.6 mm i.d., 5 μm) (Dikma Technologies Company, China) with a C_{18} guard column. The mobile phase was acetonitrile: water (40: 60:, v/v). The flow rate was 1 mL/min, and detection wavelength was set in the range of 190−400 nm (monitoring wavelength 230 nm). The results indicated that more than 45% (9.1 mg) of the NH_2-THP was coupled on the sepharose CL-4B. The beads were finally stored in 50 mM acetate buffer (pH 4.0) containing 20% ethanol at 4 °C.

2.5. Affinity Enrichment and Sample Preparation for Chemical Proteomic Study. The striatum sample was homogenized in 1 mL of lysis buffer (50 mM Tris-HCl, pH 7.5, 0.25% v/v Triton X-100, 1 mM PMSF, 1 mM DTT, 1× protease inhibitor cocktail) at 4 °C and centrifuged at 20 000 rpm for 30 min at 4 °C. The supernatant was collected and the protein concentration was determined by the Bradford method, and the concentration was adjusted to 1 mg/mL with lysis buffer. The beads were conditioned and washed three times in the binding buffer (50 mM Tris-HCl, pH 7.5, 0.25% v/v Triton X-100, 1 mM DTT, 1× protease inhibitor cocktail) prior to the incubation. Then the incubation experiments were divided into two groups (a, Blank_THPs; b, THP_THPs): (a) Protein solution (1 mL) was incubated with binding buffer for 30 min at 4 °C; (b) protein solution (1 mL) was incubated with L-THP (100 mM in binding buffer) for 30 min at 4 °C. Then the mixtures were incubated with 20 mg of beads for 3 h at 4 °C. Following incubation, beads were collected by centrifugation for 2 min at 3000 rpm. Then the beads were washed four times with the binding buffer and washing buffer (200 mM NaCl, 50 mM Tris-HCl, pH 7.5, 0.25% v/v Triton X-100, 1 mM DTT, 1× protease inhibitor cocktail), respectively, and twice with 50 mM Tris-HCl (pH 7.5) and SpeedVaced (Thermo, Milford, MA). For on-beads digestion, the gels were resuspended in 100 μL of denature buffer (8 M urea, 50 mM Tris-HCl, pH 8.3). The sample were then mixed with 2 μL of 1 M DTT and incubated at 37 °C for 2 h. Then, 10 μL of 1 M IAA was added and incubated for 40 min in dark. Finally, the solution was diluted to 1 M urea with 50 mM Tris-HCl (pH 8.3) and 5 μg trypsin was added and incubated at 37 °C overnight. Then the digested mixture was desalted with a homemade C_{18} solid-phase cartridge and stored at −80 °C before 2D-nano-LC−MS/MS analysis.

2.6. 2D-nano-LC−MS/MS Analysis and Database Searching. The 2D-nano-LC−MS/MS system consisted of a quaternary Surveyor pump and an LTQ linear IT mass spectrometer equipped with a nanospray source (Thermo, San Jose,

CA). The 2D nano-LC−MS/MS analysis was carried out according to a reported method with minor modification.[22] Briefly, the tryptic samples were dissolved in 0.1% (v/v) formic acid, loaded onto a monolith strong cation exchange (SCX) column (150 μm id × 7 cm) automatically. Then a series stepwise elution with salt concentrations of 50, 100, 150, 200, 250, 300, 350, 400, 500, and 1000 mM NH_4AC were used to gradually elute peptides from the phosphate monolithic column onto the C18 analytical column. Each salt step lasts 10 min except for the last one, which lasts for 20 min after the whole system was re-equilibrated for 10 min with buffer A (0.1% formic acid water solution), the binary gradient elution with buffer A and buffer B (0.1% formic acid acetonitrile solution) (0−10 min, from 0 to 10% buffer B, 10−100 min, from 10 to 35% buffer B, 100−105 min, from 35 to 80% buffer B, 105−115 min, 80% buffer B, 115−125 min, buffer A) for reversed phase separation was applied prior to MS detection in each cycle. The temperature of the ion transfer capillary was set at 200 °C. The spray voltage was set at 1.82 kV. All MS and MS/MS spectra were acquired in the data-dependent mode. The mass spectrometer was set so that one full MS scan was followed by six MS/MS scans.

The MS/MS spectra were searched using SEQUEST (version 2.7) against a composite database including both original and reversed rat protein database of International Protein Index (ipi.rat.3.63.fasta, including 39 670 entries, http://www.ebi-.ac.uk/IPI/IPIrat.html). Cysteine residues were searched as a fixed modification of 57.0215 Da, and methionine residues were searched as a variable modification of 15.9949 Da. Peptides were searched using fully tryptic cleavage constraints and up to two missed cleavages sites were allowed for tryptic digestion. The mass tolerances are 2 Da for parent masses and 1 Da for fragment masses. Initial searching results were filtered with the following parameters as reported previously:[23,24] the Xcorr ≥ 1.8 for a singly charged peptide, 2.5 for a doubly charged peptide, and 3.5 for a triply charged peptides; the minimum ΔC_n cutoff value of 0.08.

For semiquantitative comparisons of the proteins identified, spectral counts for each identified protein from each experiment were extracted, averaged, and compared as described previously.[23−25]

2.7. Protein Validation by Western Blots. After various treatments, proteins in the whole lysate were resolved on 10% SDS-PAGE and then transferred onto nitrocellulose membrane (Schleicher & Schuell, Dassel, Germany). The membranes were blocked overnight in phosphate-buffered saline containing 10% nonfat dry milk and 0.5% Tween-20, and incubated with primary antibodies for 2 h. Horseradish peroxidase-conjugated antirabbit IgG was used as the secondary antibody. Target proteins were imaged with the ECL system (Pierce, Rockford, IL). The bands were visualized and quantified using Quantity One imaging software (Bio-Rad). The intensities of Neurabin-1 and Calcium-dependent secretion activator 1 (CAPS1) were adjusted by beta-actin intensity.

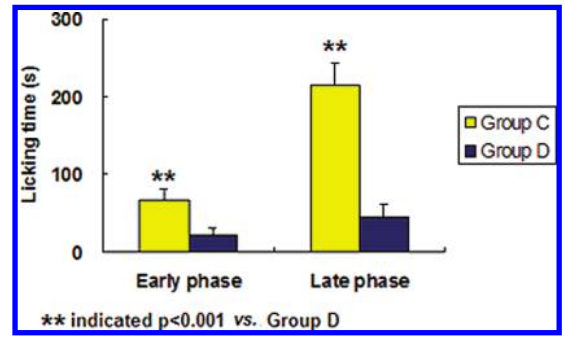

Figure 3. Effect of administration of L-THP on formalin-induced nociception in rats. Group C (CONs): vehicle + formalin injection. Group D (L-THPs): L-THP (40 mg/kg) + formalin injection. (As the injection of normal saline did not provoke nociceptive behavior, Group A (vehicle + normal saline injection) and Group B (L-THP (40 mg/kg) + normal saline injection) were not shown.)

2.8. Data Processing and Principle Component Analysis (PCA). The results of the comparative proteomics were fed into SIMCA-P for further principal component analysis (PCA). Data from the Western Blots and comparative proteomics are expressed as means ± SD and analyzed for statistical significance using Student's *t* test. $P < 0.05$ was considered significant.

3. Results

3.1. Formalin Test. The formalin-induced pain model was applied to evaluate the antinociceptive effects of L-THP. As shown in Figure 3, the licking responses evoked by formalin injection in both the early phase (0−5 min) and the late phase (15−30 min) were significantly reduced by the pretreatment of TAC (i.g.) at a single dose of 40 mg/kg.

3.2. Comparative Proteomic Analysis and Western Blots. A comprehensive shotgun proteomic profiling procedure, based on online 2D-nano-LC−MS/MS system was applied to uncover proteomic alterations associated with L-THP-induced-antinociception in the formalin test. The numbers of total spectral counts and identified proteins are listed in Table 1. For PCA of the proteins identified in the striatum of L-THP treated rats (L-THPs) and the control rats (CONs), spectral counts for each identified protein from each experiment were extracted, averaged, normalized. To improve the reliability of identification of the proteins, proteins meet the stringent filter criteria (the number of unique peptide identified more than 2; protein identified at least six out of eight rats) were included for the further Student's *t*-test statistic. A total of 152 proteins were selected based on the filter criteria and a Student's *t*-test

Table 1. Total Spectral Counts and Proteins Identified of Controls (CONs)[a] and L-THPs[b]

CONs	CONs_1	CONs_2	CONs_3	CONs_4	CONs_5	CONs_6	CONs_7	CONs_8
Total spectral counts	44508	32301	36389	39815	38709	25815	37138	39529
Total protein groups	2718	1531	1666	1949	2871	1909	1989	2420
L-THPs	L-THPs_1	L-THPs_2	L-THPs_3	L-THPs_4	L-THPs_5	L-THPs_6	L-THPs_7	L-THPs_8
Total spectral counts	40458	46835	39257	33150	41362	39119	39504	31065
Total protein groups	2602	2672	1731	2089	2799	2197	2327	2145

[a] Controls (CONs): Group C received vehicle (normal saline) 1 h prior to formalin injection. [b] L-THPs: Group D received L-THP (40 mg/kg, normal saline) 1 h prior to formalin injection. All data meet the following criteria: the Xcorr ≥ 1.8 for a singly charged peptide, 2.5 for a doubly charged peptide, and 3.5 for a triply charged peptides; the minimum ΔC_n cutoff value of 0.08.

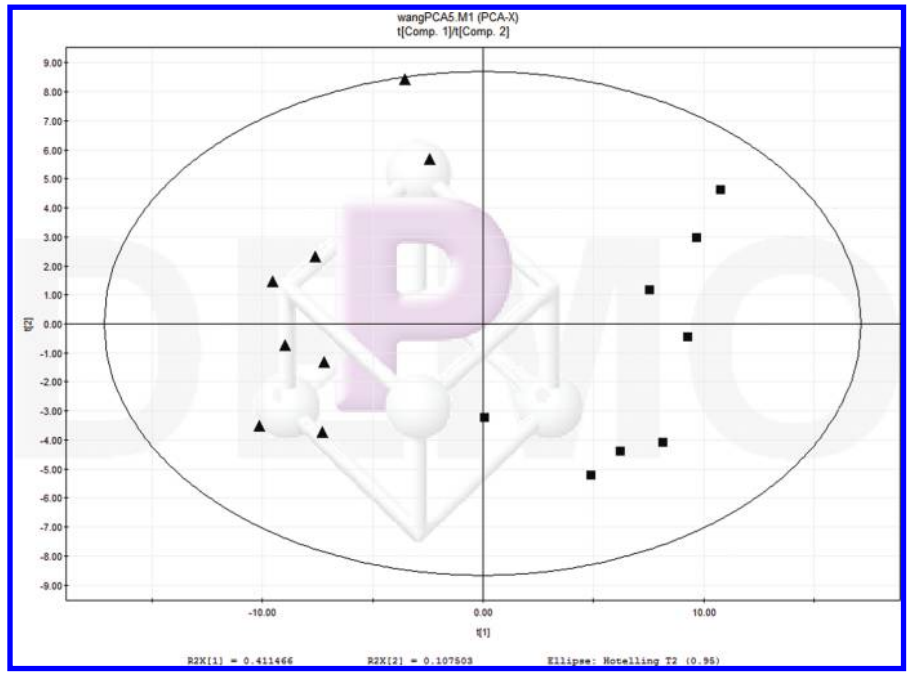

Figure 4. Score plot of PCA performed on the spectral count data of L-THPs and CONs (Box, L-THPs; Triangle, CONs). Proteins meet the following filter criteria were included for PCA: (1) the number of unique peptide identified more than 2; (2) protein identified at least six out of eight rats; (3) statistical significance ($p < 0.05$) were obtained by Student's *t*-test (L-THPs vs CONs).

Table 2. Lists of the Identified Differentially Expressed Proteins[a]

protein name	average spectral count[b]		
	CONs[c]	L-THPs[d]	ratio[e]
Ion transport			
Cacna2d1 Voltage-dependent calcium channel subunit alpha-2/delta-1	1.50 ± 2.07	7.00 ± 6.21	4.67
CAPS1 Calcium-dependent secretion activator 1	17.63 ± 9.31	4.88 ± 7.24	0.28
Slc4a4 Isoform 1 of Electrogenic sodium bicarbonate cotransporter 1	21.88 ± 16.83	5.00 ± 10.69	0.23
Vesicular trafficking and neurotransmitter release			
Rab8b Ras-related protein Rab-8B	1.50 ± 2.98	16.88 ± 11.47	11.25
Rab15 Ras-related protein Rab-15	0.75 ± 1.75	5.75 ± 2.43	7.67
Rab18 Ras-related protein Rab-18	1.50 ± 1.60	6.38 ± 3.70	4.25
Ppp1r9a Neurabin-1	2.50 ± 3.38	7.50 ± 3.46	3.00
Ngef Ephexin-1	1.88 ± 1.96	6.13 ± 3.52	3.26
Atp6v1f V-type proton ATPase subunit F	5.50 ± 4.24	1.38 ± 1.60	0.25
Energy metabolism			
Ndufv3-ps1;Ndufv3 NADH dehydrogenase (ubiquinone) flavoprotein 3-like isoform 1	1.25 ± 1.39	5.75 ± 2.38	4.60
Atp5i ATP synthase subunit e, mitochondrial	1.88 ± 3.48	6.75 ± 4.40	3.60
Others			
H2afx H2A histone family, member X	0.20 ± 0.00	19.13 ± 9.09	95.63
Rab6b RAB6B, member RAS oncogene family	1.50 ± 1.31	6.38 ± 3.16	4.25
Ncam2 91 kDa protein	1.75 ± 3.41	6.38 ± 4.81	3.64
Psmd6 Proteasome (Prosome, macropain) 26S subunit, non-ATPase, 6	1.63 ± 2.07	5.63 ± 3.46	3.46
RGD1310016 similar to CG9063-PA	9.38 ± 5.40	1.13 ± 2.10	0.12
LOC690102 hypothetical protein LOC690102	10.25 ± 7.25	0.20 ± 0.00	0.02

[a] Complete data set of identified proteins is available in Supporting Information 2. [b] Raw spectral counts values from the CONs and L-THPs were averaged. Data from eight independent experiments are expressed as means ± SD. [c] Controls (CONs): Group C received vehicle (normal saline) 1 h prior to formalin injection. [d] L-THPs: Group D received L-THP (40 mg/kg, normal saline) 1 h prior to formalin injection. [e] Ratio averaged L-THPs to CONs spectral counts. The spectral counts of zero were changed to 0.2 to avoid division by zero.

statistic ($p < 0.05$). PCA was performed on this data set, which reveals two distinct clusters corresponding to L-THPs and CONs (Figure 4). The proteins (listed in Table 2) meet the following filter criteria: (a) for the average spectral of L-THPs and CONs, the larger value more than 4;[26] (b) the spectral count ratio more than 3-fold were included for the further functional discussion. Two proteins were randomly selected from whose antibodies are commercially available and their expression levels were

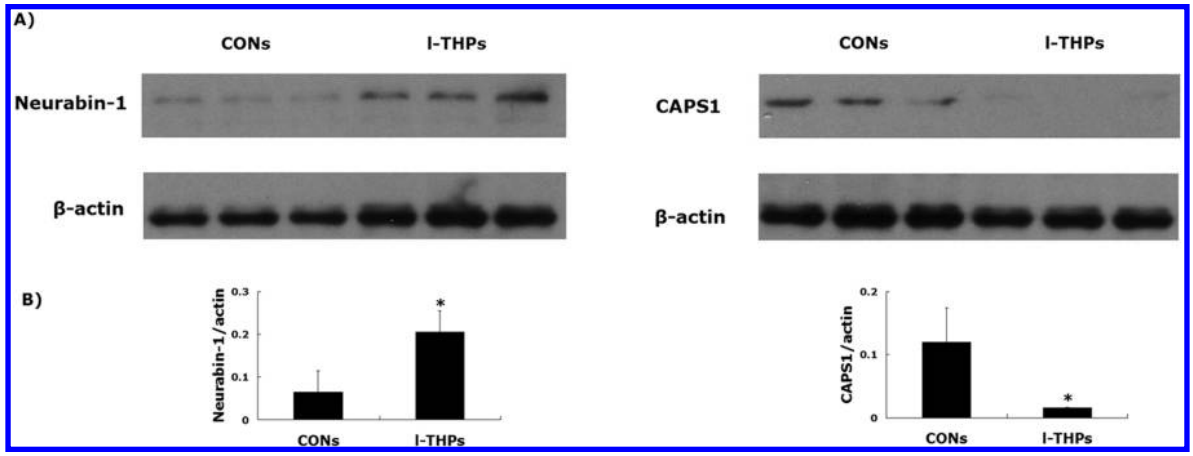

Figure 5. (A) Modulation of CAPS1 and Neurabin-1 by L-THP treatment in formalin-induced pain rats. (B) Data shown are the results of three different experiments and are represented as the relative densities of protein bands normalized to β-actin. Results are presented as means ± SD of three assays. *Significant difference compared with control ($p < 0.05$)

Table 3. Total Spectral Counts and Proteins Identified of THP_THPs[a] and Blank_THPs[b] by Chemical Proteomics[c]

sample name	total spectral counts	total identified proteins
THP_THP_1	1856	269
THP_THP_2	2378	318
THP_THP_3	1436	218
Blank_THP_1	2409	302
Blank_THP_2	2802	351
Blank_THP_3	2340	297

[a] THP_THPs: Protein solution (1 mL) was incubated with L-THP (100 mM in binding buffer) for 30 min at 4 °C. Then the mixtures were incubated with 20 mg of beads for 3 h at 4 °C. [b] Blank_THPs: Protein solution (1 mL) was incubated with binding buffer for 30 min at 4 °C. Then the mixtures were incubated with 20 mg of beads for 3 h at 4 °C. [c] All data meet the following criteria: the Xcorr ≥ 1.8 for a singly charged peptide; 2.5 for a doubly charged peptide; and 3.5 for a triply charged peptides; the minimum ΔC_n cutoff value of 0.08.

further confirmed by Western Blots. Figure 5 shows that the altered intensity of the proteins matched well with the differences obtained in 2D-nano-LC−MS/MS based proteomic analysis.

3.3. Chemical Proteomic Analysis. The numbers of total spectral counts and identified proteins identified by chemical proteomics are listed in Table 3. The proteins meet the following filter criteria: (a) the number of unique peptide identified more than 2; (b) the spectral count ratio was more than 5-fold were included for the further functional discussion. These proteins are listed in Table 4.

4. Discussions

The formalin test of chemical/inflammatory pain produces well-characterized, biphasic recuperative behaviors in rodent.[27] Acute/early phase behaviors are due to direct chemical stimulation of peripheral nociceptors whereas tonic/late phase are thought to be due to central sensitization and/or ongoing inflammatory input.[28] The antinociceptive effect of L-THP was shown in the first and second phases of the formalin test.

Two separation strategies are widely employed in current proteomics studies. One is to use one-dimensional (1D) or two-dimensional (2D) gel electrophoresis, followed by LC−MS/MS or MALDI-TOF-MS experiments. However, this approach is labor intensive with a correspondingly low throughput. Poor recovery of large or hydrophobic proteins is frequent and loss of proteins during gel separation is another drawback. Another strategy is to use multidimensional LC coupled with MS for analysis.[29] Strong cation-exchange (SCX) chromatography is widely used for protein prefractionation due to its good orthogonality to reversed phase (RP) chromatography. However, the automatic sample loading is limited because of the high back pressure of the traditional packed SCX column,and a monolithic column is a good alternative to packed one. In the present study, a phosphate monolithic capillary column was used, and because of its low back pressure, the automatic sample injection at a high flow rate could be easily realized. The 2D-nano-LC−MS/MS system applied is fully automated and displays advantages such as minimal loss of sample, no via contamination, and no sample dilution.[22]

The proteomic approach is widely applied nowadays in understanding the molecular bases of pain and identification of new targets for therapeutics.[30,31] However, traditional comparative proteomics methodology provides information for abundant proteins but only provides limited information for proteins with low abundance.[13,14] Chemical proteomics, which used small molecules as baits to fish for interacting proteins, can greatly reduce the complexity of a certain proteome and thus enhance the ability to detect and to characterize low-abundance proteins. Identification of drug-target interactions by chemical proteomics provides a means for functional annotation of previously uncharacterized proteins.[32,33] Like any other technology, chemical proteomics has strengths and weaknesses. Given many proteins that were fished out using chemical proteomics, it was puzzling that some proteins such as dopamine receptors failed to survive our stringent filter criteria, although their presence would be expected from the predicted targets of L-THP.[34] There are some possible explanations for this paradox. On one hand, the abundance of these proteins might be too low, so that they failed to be enriched in the presence of other high abundance counterparts. On the other hand, membrane-bound receptors such as serotonin and dopamine receptors are noticeably absent in the affinity chromatography sets, which can partly be explained by the experimental setup, such as the solubility and the stability of these proteins in the lysis buffer.[35] In the present study, the combined comparative and chemical proteomics were applied for understanding the mechanisms of L-THP-induced antinociception in formalin test. We found that: (1) the proteins identified by comparative proteomics are totally different from

Table 4. Lists of the Identified Proteins by Chemical Proteomics[a]

protein name	average spectral count[b] Blank_THPs[c]	THP_THPs[d]	ratio[e]
Ion transport			
Atp2b4 Isoform XA of Plasma membrane calcium-transporting ATPase 4	11.00 ± 5.56	1.00 ± 1.73	11.00
Vesicular trafficking and neurotransmitter release			
Eef1a2 Elongation factor 1-alpha 2	6.33 ± 3.06	0.20 ± 0.00	31.67
Ppp1cc Isoform Gamma-1 of Serine/threonine-protein phosphatase PP1-gamma catalytic subunit	5.67 ± 2.52	0.20 ± 0.00	28.33
Tcp1 T-complex protein 1 subunit alpha	3.33 ± 2.52	0.20 ± 0.00	16.67
Pacsin2 Isoform 4 of Protein kinase C and casein kinase substrate in neurons 2 protein	3.00 ± 2.65	0.20 ± 0.00	15.00
Agrn Isoform 3 of Agrin	3.00 ± 2.65	0.33 ± 0.00	9.00
Dgkb Diacylglycerol kinase beta	4.33 ± 0.58	0.67 ± 0.00	6.50
Dnm3 Isoform 6 of Dynamin-3	36.33 ± 10.50	6.67 ± 11.54	5.45
Others			
Fam164a Similar to RIKEN cDNA 3110050N22	4.00 ± 1.00	0.67 ± 0.58	6.00

[a] Complete data set of identified proteins is available in Supporting Information 3. [b] Raw spectral counts values from the Blank_THPs and THP_THPs were averaged. Data from eight independent experiments are expressed as means ± SD. [c] Blank_THPs: Protein solution (1 mL) was incubated with binding buffer for 30 min at 4 °C. Then the mixtures were incubated with 20 mg of beads for 3 h at 4 °C. [d] THP_THPs: Protein solution (1 mL) was incubated with L-THP (100 mM in binding buffer) for 30 min at 4 °C. Then the mixtures were incubated with 20 mg of beads for 3 h at 4 °C. [e] Ratio averaged Blank_THPs to THP-THPs spectral counts. The spectral counts of zero were changed to 0.2 to avoid division by zero.

those identified by chemical proteomics, (2) the proteins identified by comparative and chemical proteomics have interrelations, as we pointed out in the following discussion. The results indicated that comparative and chemical proteomics are quite complementary.

Dopamine is a catecholamine neurotransmitter that is best known for its roles in movement and cognition. Recently, the roles of dopamine in pain perception have been referred to in a number of investigations[36−38] and the central roles for dopaminergic neurotransmission in modulating pain perception have been reviewed.[39,40] Neurotransmitters secretion is mediated by filling, docking, priming, and fusion of vesicles with plasma membrane, and these processes are tightly regulated and involve many vesicles- and membrane-associated proteins. Calcium-dependent activator protein for secretion 1 (CAPS1) (down-regulated), a 145-kDa protein, is an evolutionarily conserved, presynaptic calcium binding protein that functions in late-stage exocytosis and in the secretion of a subset of neurotransmitters.[41,42] CAPS1 is required for the release of LDCVs that rapidly releasable and tightly coupled to Ca^{2+} influx.[43−45] Both pull down and coimmunoprecipitation assays confirmed the interration between CAPS1 and the D2 receptor. CAPS1 interacts with the D2 dopamine receptor and disruption of this interaction causes a selective decrease in dopamine release in PC12 cells.[42] THP can inhibit dopamine release in amygdaloid to inhibit an epileptic attack in rats.[46] Intermittent tail-shock stress can increase dopamine concentration in striatum.[47] Therefore, L-THP might disrupt the DA/CAPS1 interaction to decrease dopamine release in striatum to produce antinociception. Elongation factors (EF) (L-THP interacted) are highly associated with cytoskeleton, centrosphere and mitotic apparatus.[48,49] These novel activities of elongation factors have been thought to be closely related to important cellular process such as signal transduction, microtubule reorganization and cytoskeletal structures function.[50,51] The functions of EF 1 have been reviewed.[48] EF-1α is a ubiquitous and abundant protein that can bind F-actin.[52] Furthermore, EF-1α is also an activator of a PI 4-kinase that binds actin and increases actin binding.[53] Interestingly, EF-1α and diacylglycerol kinase (L-THP interacted), an enzyme in the phosphoinositide pathway were found to interact with L-THP by chemical proteomics. The phosphoinositide pathway is one of the downstream of the D2 receptor[54,55] which is discovered as a target for L-THP. [3] It is also reported that phosphoinositide signaling pathway is involved in biological mechanisms underlying the effect of the opiate receptor agonists and antagonists.[56] L-THP has been verified as a dopamine (DA) receptor antagonist, and it has affinity for opiate receptors.[1,2] (CAPS1) (down-regulated), elongation factors (EF) (L-THP interacted) and diacylglycerol kinase (L-THP interacted) were identified by comparative and chemical proteomics, respectively. These proteins all related with DA receptor, making the DA receptor involved in the L-THP induced antinociception more reliable. The combined comparative and chemical proteomics give more information on the mechanisms how the DA receptor involved in the L-THP induced antinociception which might through the change of the interaction of DA/CAPS1 and/or the phosphoinositide signaling pathway.

The protein serine/threonine phosphatase protein-1 (PP1) (L-THP interacted) is a ubiquitous eukaryotic enzyme that regulates a variety of cellular processes through the dephosphorylation of dozens of substrates.[57] The role of serine/threonine protein phosphatases in exocytosis has been reviewed, and the regulation of exocytosis in neurons is essential for effective neurotransmission.[58] PP1 acts as a key regulator of activity-dependent changes in synaptic function.[59,60] Neurabin-1 (up-regulated) can target PP1 activity to actin-rich structures in cultured cells to promote filopodia and disassemble the stress fiber network.[61] V-ATPase (Atp6v1f V-type proton ATPase subunit F, down-regulated) is a major proton pump in the proton homeostasis of eukaryotic. Most of the biochemistry, cell biology and physiology related to V-ATPase have been recently reviewed.[62,63] V-ATPase can establish acid pH and the electrochemical proton gradient constitutes a driving force for the accumulation of neurotransmitters and hormones into secretory vesicles. V-ATPase may also have direct roles in the regulation of vesicular trafficking.[64] Rab small GTPases (Rab 8b, Rab 15 and Rab 18, up-regulated) constitute the largest

family of the known membrane trafficking proteins.[65] It is considered a specialized mode of membrane trafficking that is achieved by docking and fusion of secretory vesicles to the plasma membrane, while secretory vesicle traffic is thought to be regulated by a family of Rab small GTPases, which are regulators of membrane traffic that are common to all eukaryotic cells.[66] In addition, Rab proteins can modulate the activity and trafficking of dopamine transporter, which is crucial regulator of dopaminergic neurotransmission by efficiently reuptaking the dopamine into the nerve terminal from the synaptic cleft.[67] Ephexin (down-regulated), a novel Eph receptor-interacting protein, is also related to presynaptic release.[68−70] T-complex protein 1 (L-THP interacted), played a role in the folding of actin, tubulin and microtubules, which had critical roles in neurotransmitter trafficking.[71,72] Pacsins are intracellular adapter proteins involved in vesicle transport, memberane dynamics and actin reorganization.[73,74] Pacsin 2 (L-THP interacted) was found to bind to dynamin, synaptojanin 1 and N-WASP via its highly conserved SH3 domains probably bind to the same proline-rich regions in these ligands[75] and therefore functions in vesicle formation and transport.[76−78] Dynamin (L-THP interacted) functions in the fission of endocytic pits in the process of clathrin-mediated endocytosis.[79,80] As synaptic vesicles store various neurotransmitters that are released at the synapse, therefore, L-THP might also affect the vesicular trafficking and neurotransmitters release to produce antinociception.

ATP, the energy currency in any cellular activity, is primarily produced in the mitochondria via the respiratory chain and is the result of two coupled process: electron transport and oxidative phosphorylation. Among different mitochondrial enzymes that undergo differential deregulation due to L-THP treatment in the formalin test, some are associated with electron transport chain and oxidative phosphorylation (NADH dehydrogenase (ubiquinone) flavoprotein 3-like isoform 1 and ATP synthase subunit e, up-regulated). Neurons use adenosine triphosphate (ATP) as an energy source to drive biochemical processes involved in various cell functions. Mitochondria in axons and presynaptic terminals provide sources of ATP to drive the ion pumps that are concentrated in these structures to rapidly restore ion gradients following depolarization and neurotransmitter release.[81] L-THP changed the energy metabolism in the formalin induced pain rats, which might associate with its antinociceptive function.

The essential functions of nociceptors of transducing noxious stimuli into depolarizations that trigger action potentials, conducting the action potentials from the peripheral sensory site to synapse in the central nervous system, and converting the action potentials into neurotransmitter release at the presynaptic terminal all depend on ion channels.[82] The Voltage-dependent calcium channel subunit alpha-2/delta-1 (up-regulated) possesses a stereoselective, high-affinity binding site for gabapentin (GBP) (1-aminomethylcyclohexane; Neurontin), widely used to treat neuralgic pain.[83,84] Plasma membrane calcium-transporting ATPase (L-THP interacted) is essential to cellular Ca^{2+} homeostasis, and therefore influences many other cellular pathways sensitive to calcium levels.[85,86] L-THP was reported to have effects on Ca^{2+} current[87,88] and the L-THP's antinociception in the formalin test might also associate with ion transport.

5. Conclusion

In conclusion, these results showed that comparative proteomics based on shotgun approach is a valuable tool for molecular mechanism studies, since it allows the simultaneously evaluate the global proteins alterations. Deregulated proteins after L-THP treatment in formalin-induced pain rats were globally identified. The proteome interacting with the fixed L-THP was identified by chemical proteomics. The results of comparative and chemical proteomics are quite complementary. Based on the results of comparative and chemical proteomics, we concluded that proteins associated with signal transduction, vesicular trafficking and neurotransmitter release, energy metabolism, and ion transport play important roles in L-THP-induced antinociception in formalin test, although the precise roles of these identified moleculars in L-THP-induced antinociception need further study. The current study improves the understanding of mechanisms of L-THP-induced antinociception, and provides prospects for the application of the combined comparative and chemical proteomics based on shotgun approach in biological mechanisms study.

Supporting Information Available: Supplemental figures and tables. This material is available free of charge via the Internet at http://pubs.acs.org.

References

(1) Sun, B. C.; Huang, K. X.; Jin, G. Z. Comparison of Effects of Tetrahydropalmatine Enantiomers on Firing Activity of Dopamine Neurons in Substantia-Nigra Pars Compacta. *Acta Pharmacol. Sin.* **1992**, *13* (4), 292–297.

(2) Hu, J. Y.; Jin, G. Z. Effect of tetrahydropalmatine analogs on Fos expression induced by formalin-pain. *Acta Pharmacol. Sin.* **1999**, *20* (3), 193–200.

(3) Chu, H. Y.; Jin, G. Z.; Friedman, E.; Zhen, X. C. Recent development in studies of tetrahydroprotoberberines: Mechanism in antinociception and drug addiction. *Cell. Mol. Neurobiol* **2008**, *28* (4), 491–499.

(4) Camps, M.; Cortes, R.; Gueye, B.; Probst, A.; Palacios, J. M. Dopamine-Receptors in Human-Brain - Autoradiographic Distribution of D2 Sites. *Neuroscience* **1989**, *28* (2), 275–290.

(5) Robertson, G. S.; Vincent, S. R.; Fibiger, H. C. D1 and D2 Dopamine-Receptors Differentially Regulate C-Fos Expression in Striatonigral and Striatopallidal Neurons. *Neuroscience* **1992**, *49* (2), 285–296.

(6) Wang, C.; Wang, S. W.; Fan, G. R.; Zou, H. F. Screening of antinociceptive components in Corydalis yanhusuo W.T. Wang by comprehensive two-dimensional liquid chromatography/tandem mass spectrometry. *Anal. Bioanal. Chem.* **2010**, *396* (5), 1731–1740.

(7) Hong, Z. Y.; Fan, G. R.; Le, J.; Chai, Y. F.; Yin, X. P.; Wu, Y. T. Brain pharmacokinetics and tissue distribution of tetrahydropalmatine enantiomers in rats after oral administration of the racemate. *Biopharm. Drug Dispos.* **2006**, *27* (3), 111–117.

(8) Zhang, Z. M.; Zheng, X. X.; Jiang, B.; Zhou, Q. Effects of L-tetrahydropalmatine on concentrations of neurotransmitter amino acids in mice with cerebral ischemia. *Zhongguo Zhong Yao Za Zhi* **2004**, *29* (4), 371–3.

(9) Aebersold, R.; Mann, M. Mass spectrometry-based proteomics. *Nature* **2003**, *422* (6928), 198–207.

(10) Hanash, S. Disease proteomics. *Nature* **2003**, *422* (6928), 226–232.

(11) Rifai, N.; Gillette, M. A.; Carr, S. A. Protein biomarker discovery and validation: the long and uncertain path to clinical utility. *Nat. Biotechnol.* **2006**, *24* (8), 971–983.

(12) Lescuyer, P.; Hochstrasser, D.; Rabilloud, T. How shall we use the proteomics toolbox for biomarker discovery. *J. Proteome Res.* **2007**, *6* (9), 3371–3376.

(13) Fonovic, M.; Bogyo, M. Activity-based probes as a tool for functional proteomic analysis of proteases. *Expert Rev. Proteomics* **2008**, *5* (5), 721–730.

(14) Greenbaum, D.; Baruch, A.; Hayrapetian, L.; Darula, Z.; Burlingame, A.; Medzihradszky, K. F.; Bogyo, M. Chemical approaches for functionally probing the proteome. *Mol. Cell. Proteomics* **2002**, *1* (1), 60–68.

(15) Salisbury, C. M.; Cravatt, B. F. Click chemistry-led advances in high content functional proteomics. *Qsar Comb. Sci.* **2007**, *26* (11−12), 1229–1238.

(16) Figeys, D. Novel approaches to map protein interactions. *Curr. Opin. Biotechnol.* **2003**, *14* (1), 119–125.

(17) Tian, R. J.; Xu, S. Y.; Lei, X. Y.; Jin, W. H.; Ye, M. L.; Zou, H. F. Characterization of small-molecule-biomicromolecule interactions: From simple to complex. *Trend. Anal. Chem.* **2005**, *24* (9), 810–825.
(18) Zimmermann, M. Ethical Guidelines for Investigations of Experimental Pain in Conscious Animals. *Pain* **1983**, *16* (2), 109–110.
(19) Santos, A. R. S.; Calixto, J. B. Further evidence for the involvement of tachykinin receptor subtypes in formalin and capsaicin models of pain in mice. *Neuropeptides* **1997**, *31* (4), 381–389.
(20) Bhakuni, D. S.; Kumar, P. Synthesis of (±)-12-Nitro & (±)-12-Amino Derivatives of Scoulerine, Coreximine, Tetrahydropalmatrubine, tetrahydropalmatine & Xylopinine. *Indian J. Chem.* **1985**, *24B*, 596–601.
(21) Tian, R. J.; Jiang, X. N.; Li, X.; Jiang, X. G.; Feng, S.; Xu, S. Y.; Han, G. H.; Ye, M. L.; Zou, H. F. Biological fingerprinting analysis of the interactome of a kinase inhibitor in human plasma by a chemiproteomic approach. *J. Chromatogr., A* **2006**, *1134* (1−2), 134–142.
(22) Wang, F. J.; Dong, J.; Jiang, X. G.; Ye, M. L.; Zou, H. F. Capillary trap column with strong cation-exchange monolith for automated shotgun proteome analysis. *Anal. Chem.* **2007**, *79* (17), 6599–6606.
(23) Roth, A. F.; Wan, J. M.; Bailey, A. O.; Sun, B. M.; Kuchar, J. A.; Green, W. N.; Phinney, B. S.; Yates, J. R.; Davis, N. G. Global analysis of protein palmitoylation in yeast. *Cell* **2006**, *125* (5), 1003–1013.
(24) Tian, R. J.; Li, L. D.; Tang, W.; Liu, H. W.; Ye, M. L.; Zhao, Z. B. K.; Zou, H. F. Chemical proteomic study of isoprenoid chain interactome with a synthetic photoaffinity probe. *Proteomics* **2008**, *8* (15), 3094–3104.
(25) Wan, J.; Roth, A. F.; Bailey, A. O.; Davis, N. G. Palmitoylated proteins: purification and identification. *Nat. Protoc.* **2007**, *2* (7), 1573–1584.
(26) Old, W. M.; Meyer-Arendt, K.; Aveline-Wolf, L.; Pierce, K. G.; Mendoza, A.; Sevinsky, J. R.; Resing, K. A.; Ahn, N. G. Comparison of label-free methods for quantifying human proteins by shotgun proteomics. *Mol. Cell. Proteomics* **2005**, *4* (10), 1487–1502.
(27) Dubuisson, D.; Dennis, S. G. Formalin Test - Quantitative Study of Analgesic Effects of Morphine, Meperidine, and Brain-Stem Stimulation in Rats and Cats. *Pain* **1977**, *4* (2), 161–174.
(28) Tjolsen, A.; Berge, O. G.; Hunskaar, S.; Rosland, J. H.; Hole, K. The Formalin Test - an Evaluation of the Method. *Pain* **1992**, *51* (1), 5–17.
(29) Chen, G.; Pramanik, B. N. Application of LC/MS to proteomics studies: current status and future prospects. *Drug Discovery Today* **2009**, *14*, 465–471.
(30) Zhang, Y.; Wang, Y. H.; Zhang, X. H.; Ge, H. Y.; Arendt-Nielsen, L.; Shao, J. M.; Yue, S. W. Proteomic analysis of differential proteins related to the neuropathic pain and neuroprotection in the dorsal root ganglion following its chronic compression in rats. *Exp. Brain Res.* **2008**, *189* (2), 199–209.
(31) Niederberger, E.; Geisslinger, G. Proteomics in Neuropathic pain research. *Anesthesiology* **2008**, *108* (2), 314–323.
(32) Saxena, C.; Zhen, E.; Higgs, R. E.; Hale, J. E. An immuno-chemo-proteomics method for drug target deconvolution. *J. Proteome Res.* **2008**, *7* (8), 3490–3497.
(33) Rix, U.; Superti-Furga, G. Target profiling of small molecules by chemical proteomics. *Nat. Chem. Biol.* **2009**, *5* (9), 616–624.
(34) Ma, Z. Z.; Xu, W.; Jensen, N. H.; Roth, B. L.; Liu-Chen, L. Y.; Lee, D. Y. W. Isoquinoline alkaloids isolated from Corydalis yanhusuo and their binding affinities at the dopamine D-1 receptor. *Molecules* **2008**, *13* (9), 2303–2312.
(35) Bender, A.; Mikhailov, D.; Glick, M.; Scheiber, J.; Davies, J. W.; Cleaver, S.; Marshall, S.; Tallarico, J. A.; Harrington, E.; Cornella-Taracido, I.; Jenkins, J. L. Use of Ligand Based Models for Protein Domains To Predict Novel Molecular Targets and Applications To Triage Affinity Chromatography Data. *J. Proteome Res.* **2009**, *8* (5), 2575–2585.
(36) Lopez-Avila, A.; Coffeen, U.; Ortega-Legaspi, J. M.; del Angel, R.; Pellicer, F. Dopamine and NMDA systems modulate long-term nociception in the rat anterior cingulate cortex. *Pain* **2004**, *111* (1−2), 136–143.
(37) Hagelberg, N.; Martikainen, I. K.; Mansikka, H.; Hinkka, S.; Nagren, K.; Hietala, J.; Scheinin, H.; Pertovaara, A. Dopamine D2 receptor binding in the human brain is associated with the response to painful stimulation and pain modulatory capacity. *Pain* **2002**, *99* (1−2), 273–279.
(38) Pertovaara, A.; Martikainen, I. K.; Hagelberg, N.; Mansikka, H.; Nagren, K.; Hietala, J.; Scheinin, H. Striatal dopamine D2/D3 receptor availability correlates with individual response characteristics to pain. *Eur. J. Neurosci.* **2004**, *20* (6), 1587–1592.
(39) Wood, P. B. Role of central dopamine in pain and analgesia. *Expert Rev. Neurother.* **2008**, *8* (5), 781–97.
(40) Potvin, S.; Grignon, S.; Marchand, S. Human Evidence of a Supra-Spinal Modulating Role of Dopamine on Pain Perception. *Synapse* **2009**, *63* (5), 390–402.
(41) Ann, K.; Kowalchyk, J. A.; Loyet, K. M.; Martin, T. F. J. Novel Ca2+-binding protein (CAPS) related to UNC-31 required for Ca2+-activated exocytosis. *J. Biol. Chem.* **1997**, *272* (32), 19637–19640.
(42) Binda, A. V.; Kabbani, N.; Levenson, R. Regulation of dense core vesicle release from PC12 cells by interaction between the D2 dopamine receptor and calcium-dependent activator protein for secretion (CAPS). *Biochem. Pharmacol.* **2005**, *69* (10), 1451–1461.
(43) Elhamdani, A.; Martin, T. F. J.; Kowalchyk, J. A.; Artalejo, C. R. Ca2+-dependent activator protein for secretion is critical for the fusion of dense-core vesicles with the membrane in calf adrenal chromaffin. *J. Neurosci.* **1999**, *19* (17), 7375–7383.
(44) Liu, Y. Y.; Schirra, C.; Stevens, D. R.; Matti, U.; Speidel, D.; Hof, D.; Bruns, D.; Brose, N.; Rettig, J. CAPS facilitates filling of the rapidly releasable pool of large dense-core vesicles. *J. Neurosci.* **2008**, *28* (21), 5594–5601.
(45) Berwin, B.; Floor, E.; Martin, T. F. J. CAPS (mammalian UNC-31) protein localizes to membranes involved in dense-core vesicle exocytosis. *Neuron* **1998**, *21* (1), 137–145.
(46) Chang, C. K.; Lin, M. T. DL-Tetrahydropalmatine may act through inhibition of amygdaloid release of dopamine to inhibit an epileptic attack in rats. *Neurosci. Lett.* **2001**, *307* (3), 163–166.
(47) Abercrombie, E. D.; Keefe, K. A.; Difrischia, D. S.; Zigmond, M. J. Differential Effect of Stress on In Vivo Dopamine Release in Striatum, Nucleus Accumbens, and Medial Frontal Cortex. *J. Neurochem.* **1989**, *52*, 1655–1658.
(48) Ejiri, S. Moonlighting functions of polypeptide elongation factor 1: From actin bundling to zinc finger protein R1-associated nuclear localization. *Biosci. Biotechnol. Biochem.* **2002**, *66* (1), 1–21.
(49) Kuriyama, R.; Savereide, P.; Lefebvre, P.; Dasgupta, S. The Predicted Amino-Acid-Sequence of a Centrosphere Protein in Dividing Sea-Urchin Eggs Is Similar to Elongation-Factor (Ef-1-Alpha). *J. Cell Sci.* **1990**, *95*, 231–236.
(50) Bassell, G. J.; Powers, C. M.; Taneja, K. L.; Singer, R. H. Single Messenger-Rnas Visualized by Ultrastructural in-Situ Hybridization Are Principally Localized at Actin Filament Intersections in Fibroblasts. *J. Cell Biol.* **1994**, *126* (4), 863–876.
(51) Shiina, N.; Gotoh, Y.; Kubomura, N.; Iwamatsu, A.; Nishida, E. Microtubule Severing by Elongation-Factor 1-Alpha. *Science* **1994**, *266* (5183), 282–285.
(52) Yang, F.; Demma, M.; Warren, V.; Dharmawardhane, S.; Condeelis, J. Identification of an Actin-Binding Protein from Dictyostelium as Elongation Factor-1a. *Nature* **1990**, *347* (6292), 494–496.
(53) Yang, W.; Boss, W. F. Regulation of Phosphatidylinositol 4-Kinase by the Protein Activator Pik-A49 - Activation Requires Phosphorylation of Pik-A49. *J. Biol. Chem.* **1994**, *269* (5), 3852–3857.
(54) Nair, V. D.; Sealfon, S. C. Agonist-specific transactivation of phosphoinositide 3-kinase signaling pathway mediated by the dopamine D-2 receptor. *J. Biol. Chem.* **2003**, *278* (47), 47053–47061.
(55) Nair, V. D.; Olanow, C. W.; Sealfon, S. C. Activation of phosphoinositide 3-kinase by D-2 receptor prevents apoptosis in dopaminergic cell lines. *Biochem. J.* **2003**, *373*, 25–32.
(56) Agadjanov, M. I.; Vartanian, G. S.; Tadevosyan, Y. V.; Batikyan, T. B.; Agadjanova, E. M. Possible role of the phosphoinositide pathway for signal transduction in changes in the sensitivity of delta-opiate receptors during diabetes mellitus B. *Exp. Biol. Med.* **2004**, *137* (2), 147–149.
(57) Ceulemans, H.; Bollen, M. Functional diversity of protein phosphatase-1, a cellular economizer and reset button. *Physiol. Rev.* **2004**, *84* (1), 1–39.
(58) Sim, A. T. R.; Baldwin, M. L.; Rostas, J. A. P.; Holst, J.; Ludowyke, R. I. The role of serine/threonine protein phosphatases in exocytosis. *Biochem. J.* **2003**, *373*, 641–659.
(59) Blitzer, R. D.; Conner, J. H.; Brown, G. P.; Wong, T.; Shenolikar, S.; Iyengar, R.; Landau, E. M. Gating of CaMKII by cAMP-regulated protein phosphatase activity during LTP. *Science* **1998**, *280* (5371), 1940–1943.
(60) Mulkey, R. M.; Endo, S.; Shenolikar, S.; Malenka, R. C. Involvement of a Calcineurin/Inhibitor-1 Phosphatase Cascade in Hippocampal Long-Term Depression. *Nature* **1994**, *369* (6480), 486–488.
(61) Oliver, C. J.; Terry-Lorenzo, R. T.; Elliott, E.; Bloomer, W. A. C.; Li, S.; Brautigan, D. L.; Colbran, R. J.; Shenolikar, S. Targeting protein phosphatase 1 (PP1) to the actin cytoskeleton: the neurabin I/PP1 complex regulates cell morphology. *Mol. Cell. Biol.* **2002**, *22* (13), 4690–4701.
(62) Forgac, M. Vacuolar ATPases: rotary proton pumps in physiology and pathophysiology. *Nat. Rev. Mol. Cell Biol.* **2007**, *8* (11), 917–929.

(63) Nishi, T.; Forgac, M. The vacuolar (H+)-atpases - Nature's most versatile proton pumps. *Nat. Rev. Mol. Cell Biol.* **2002**, *3* (2), 94–103.
(64) Marshansky, V.; Futai, M. The V-type H+-ATPase in vesicular trafficking: targeting, regulation and function. *Curr. Opin. Cell Biol.* **2008**, *20* (4), 415–426.
(65) Zerial, M.; McBride, H. Rab proteins as membrane organizers. *Nat. Rev. Mol. Cell Biol.* **2001**, *2* (2), 107–117.
(66) Fukuda, M. Regulation of secretory vesicle traffic by Rab small GTPases. *Cell. Mol. Life Sci.* **2008**, *65* (18), 2801–2813.
(67) Furman, C. A.; Lo, C. B.; Stokes, S.; Esteban, J. A.; Gnegy, M. E. Rab 11 regulates constitutive dopamine transporter trafficking and function in N2A neuroblastoma cells. *Neurosci. Lett.* **2009**, *463* (1), 78–81.
(68) Frank, C. A.; Pielage, J.; Davis, G. W. A Presynaptic Homeostatic Signaling System Composed of the Eph Receptor, Ephexin, Cdc42, and Ca(V)2.1 Calcium Channels. *Neuron* **2009**, *61* (4), 556–569.
(69) Knoll, B.; Drescher, U. Src family kinases are involved in EphA receptor-mediated retinal axon guidance. *J. Neurosci.* **2004**, *24* (28), 6248–6257.
(70) Shamah, S. M.; Lin, M. Z.; Goldberg, J. L.; Estrach, S.; Sahin, M.; Hu, L.; Bazalakova, M.; Neve, R. L.; Corfas, G.; Debant, A.; Greenberg, M. E. EphA receptors regulate growth cone dynamics through the novel guanine nucleotide exchange factor ephexin. *Cell* **2001**, *105* (2), 233–244.
(71) Yaffe, M. B.; Farr, G. W.; Miklos, D.; Horwich, A. L.; Sternlicht, M. L.; Sternlicht, H. Tcp1 Complex Is a Molecular Chaperone in Tubulin Biogenesis. *Nature* **1992**, *358* (6383), 245–248.
(72) Ursic, D.; Sedbrook, J. C.; Himmel, K. L.; Culbertson, M. R. The Essential Yeast Tcp1 Protein Affects Actin and Microtubules. *Mol. Biol. Cell* **1994**, *5* (10), 1065–1080.
(73) Grimm-Gunter, E. M. S.; Milbrandt, M.; Merkl, B.; Paulsson, M.; Plomann, M. PACSIN proteins bind tubulin and promote microtubule assembly. *Exp. Cell Res.* **2008**, *314* (10), 1991–2003.
(74) Ritter, B.; Modregger, J.; Paulsson, M.; Plomann, M. PACSIN 2, a novel member of the PACSIN family of cytoplasmic adapter proteins. *Febs Lett.* **1999**, *454* (3), 356–362.
(75) Modregger, J.; Ritter, B.; Witter, B.; Paulsson, M.; Plomann, M. All three PACSIN isoforms bind to endocytic proteins and inhibit endocytosis. *J. Cell Sci.* **2000**, *113* (24), 4511–4521.
(76) Cremona, O.; Di Paolo, G.; Wenk, M. R.; Luthi, A.; Kim, W. T.; Takei, K.; Daniell, L.; Nemoto, Y.; Shears, S. B.; Flavell, R. A.; McCormick, D. A.; De Camilli, P. Essential role of phosphoinositide metabolism in synaptic vesicle recycling. *Cell* **1999**, *99* (2), 179–188.
(77) Miki, H.; Sasaki, T.; Takai, Y.; Takenawa, T. Induction of filopodium formation by a WASP-related actin-depolymerizing protein N-WASP. *Nature* **1998**, *391* (6662), 93–96.
(78) Miki, H.; Miura, K.; Takenawa, T. N-WASP, a novel actin-depolymerizing protein, regulates the cortical cytoskeletal rearrangement in a PIP2-dependent manner downstream of tyrosine kinases. *Embo J.* **1996**, *15* (19), 5326–5335.
(79) Lu, W. B.; Ma, H.; Sheng, Z. H.; Mochida, S. Dynamin and Activity Regulate Synaptic Vesicle Recycling in Sympathetic Neurons. *J. Biol. Chem.* **2009**, *284* (3), 1930–1937.
(80) Newton, A. J.; Kirchhausen, T.; Murthy, V. N. Inhibition of dynamin completely blocks compensatory synaptic vesicle endocytosis. *Proc. Natl. Acad. Sci. U.S.A.* **2006**, *103* (47), 17955–17960.
(81) Mattson, M. P.; Liu, D. Energetics and oxidative stress in synaptic plasticity and neurodegenerative disorders. *Neuromol. Med.* **2002**, *2* (2), 215–231.
(82) McCleskey, E. W.; Gold, M. S. Ion channels of nociception. *Annu. Rev. Physiol.* **1999**, *61*, 835–856.
(83) Fuller-Bicer, G. A.; Varadi, G.; Koch, S. E.; Ishii, M.; Bodi, I.; Kadeer, N.; Muth, J. N.; Mikala, G.; Petrashevskaya, N. N.; Jordan, M. A.; Zhang, S. P.; Qin, N.; Flores, C. M.; Isaacsohn, I.; Varadi, M.; Mori, Y.; Jones, W. K.; Schwartz, A. Targeted disruption of the voltage-dependent calcium channel alpha(2)/delta-1-subunit. *Am. J. Physiol.-Heart C.* **2009**, *297* (1), H117–H124.
(84) Narita, M.; Nakajima, M.; Miyoshi, K.; Narita, M.; Nagumo, Y.; Miyatake, M.; Yajima, Y.; Yanagida, K.; Yamazaki, M.; Suzuki, T. Role of spinal voltage-dependent calcium channel alpha(2)delta-1 subunit in the expression of a neuropathic pain-like state in mice. *Life Sci.* **2007**, *80* (22), 2015–2024.
(85) Carafoli, E.; Brini, M. Calcium pumps: structural basis for and mechanism of calcium transmembrane transport. *Curr. Opin. Chem. Biol.* **2000**, *4* (2), 152–161.
(86) Carafoli, E.; Stauffer, T. The Plasma-Membrane Calcium-Pump - Functional Domains, Regulation of the Activity, and Tissue-Specificity of Isoform Expression. *J. Neurobiol.* **1994**, *25* (3), 312–324.
(87) Chan, P.; Chiu, W. T.; Chen, Y. J.; Wu, P. J.; Cheng, J. T. Calcium influx inhibition: Possible mechanism of the negative effect of tetrahydropalmatine on left ventricular pressure in isolated rat heart. *Planta Med.* **1999**, *65* (4), 340–342.
(88) Huang, K.; Dai, G. Z.; Li, X. H.; Fan, Q.; Cheng, L.; Feng, Y. B.; Xia, G. J.; Yao, W. X. Blocking L-calcium current by l-tetrahydropalmatine in single ventricular myocyte of guinea pigs. *Acta Pharmacol. Sin.* **1999**, *20* (10), 907–911.

PR1001274